A SEGMENTED DISH PHOTOVOLTAIC CONCENTRATOR

by

Mark Steven Swenson

A Thesis Submitted to the Faculty of the

DEPARTMENT OF ELECTRICAL ENGINEERING

In Partial Fulfillment of the Requirements
For the Degree of

MASTER OF SCIENCE

In the Graduate College

THE UNIVERSITY OF ARIZONA

1 9 8 0

STATEMENT BY AUTHOR

This thesis has been submitted in partial fulfillment of requirements for an advanced degree at The University of Arizona and is deposited in The University Library to be made available to borrowers under rules of the Library.

Brief quotations from this thesis are allowable without special permission, provided that accurate acknowledgment of source is made. Requests for permission for extended quotation from or reproduction of this manuscript in whole or in part may be granted by the head of the major department of the Dean of the Graduate College when in his judgement the proposed use of the material is in the interests of scholarship. In all other instances, however, permission must be obtained from the author.

SIGNED: Mark S. Swenson

APPROVAL BY THESIS DIRECTOR

This thesis has been approved on the date shown below:

Reginald L. Call
REGINALD L. CALL
Associate Professor of
Electrical Engineering

21 Dec 1979
Date

PREFACE

Photovoltaic solar cells in segmented dish concentrators have future promise for efficiently delivering electrical power at a relatively low cost. In this project, several concentrators were assembled and several aspects of their performance were studied. Considerable experience was gained in developing techniques for mounting cells in concentrators. Also, knowledge was aquired for improving the overall performance of the concentrator.

I would like to gratefully thank my advisor, Dr. R. L. Call, for his assistance and helpful suggestions. I am also indebted to Mr. W. Meinel of Arizona Scientific Research, Tucson, Arizona for providing the receiver and optical module components of the concentrator. I would also like to acknowledge Sandia Laboratories of Albuquerque, New Mexico who funded the project (Sandia Contract No. 13 - 0211).

TABLE OF CONTENTS

LIST OF TABLES

LIST OF ILLUSTRATIONS

ABSTRACT

Prior to mounting solar cells in concentrators, methods of mounting the cells were thoroughly investigated. In order to make electrical contact to the back sides of the cells, they were first mounted onto molybdenum substrates. Experiments were conducted to select an adhesive for mounting the cell-substrate combinations onto the receivers. Silicone rubber was chosen because of its thermally conductive, electrically insulating characteristics. I-V characteristic curves of the completed modules were plotted using an X-Y recorder. The electrical data was used to evaluate the module performance and determine how improvements could be made. Thermocouples were also used to monitor cell temperatures to determine the efficiency of the various heat sinking techniques.

CHAPTER I

INTRODUCTION

In the last few years the need to develop alternate sources of energy has become very evident. Solar energy in particular appears to have a bright future. One method of collecting solar energy is through the use of photovoltaic solar cells which convert light into direct electrical current.

Why Solar Concentrators

Solar concentrators can be very effective in reducing the area on which light is to be collected. There are several reasons why this may be desirable. In thermal applications higher temperatures can be achieved through the use of concentrators. In photovoltaic applications more electrical power can be generated by solar cells when concentrated light is focused on the cells. The current and power generated by solar cells are both proportional to the intensity of the incoming light and the surface area of the given cells. Thus, the generated electrical power can be increased by using more concentrated light or by adding more solar cells to the given system. Due to the high cost of photovoltaic solar cells it can quickly become very expensive to add more cells to a system. In many instances it is much more economical to use a limited number of solar cells and light that is very concentrated. Although a concentrator is an extra cost, the reduced cost of solar cells can make

up this difference if the concentrator is comparatively inexpensive. Under these circumstances solar concentrators become very cost effective.

Cell Parameters and Equations

Photovoltaic solar cells are comprised of two layers of semiconductor material, an n-type layer and a p-type layer. The cells used in this project are single crystal silicon cells. The cells have been doped appropriately to form a p-n junction. The thin n-type layer lies on top of the p-type layer. Electron-hole pairs are generated in the semiconductor when the absorbed photons have energies greater than the band gap energy of silicon. If minority carriers reach the junction before they recombine they will be swept across the junction by the depletion electric field giving rise to a photo generated electric field, opposite in direction to the depletion electric field. Ohmic contacts are attached to each side of the junction to collect the generated current. The front or top contact has a grid structure in order to allow the light to penetrate into the junction. The back contact covers the complete back side of the cell. The basic elements of a solar cell are shown in Figure 1.

An equivalent circuit of a solar cell is shown in Figure 2. The circuit is composed of an ideal current source I_L, the diode of the junction, a series resistance R_s, and a shunt resistance R_{sh}. R_L is the load resistance which is external to the cell itself. The value of I_L is proportional to the light intensity. These elements are related through equation (1).

$$I = \frac{V-IR_s}{R_{sh}} + I_s\left\{\exp(BV-BIR_s) - 1\right\} - I_L \qquad (1)$$

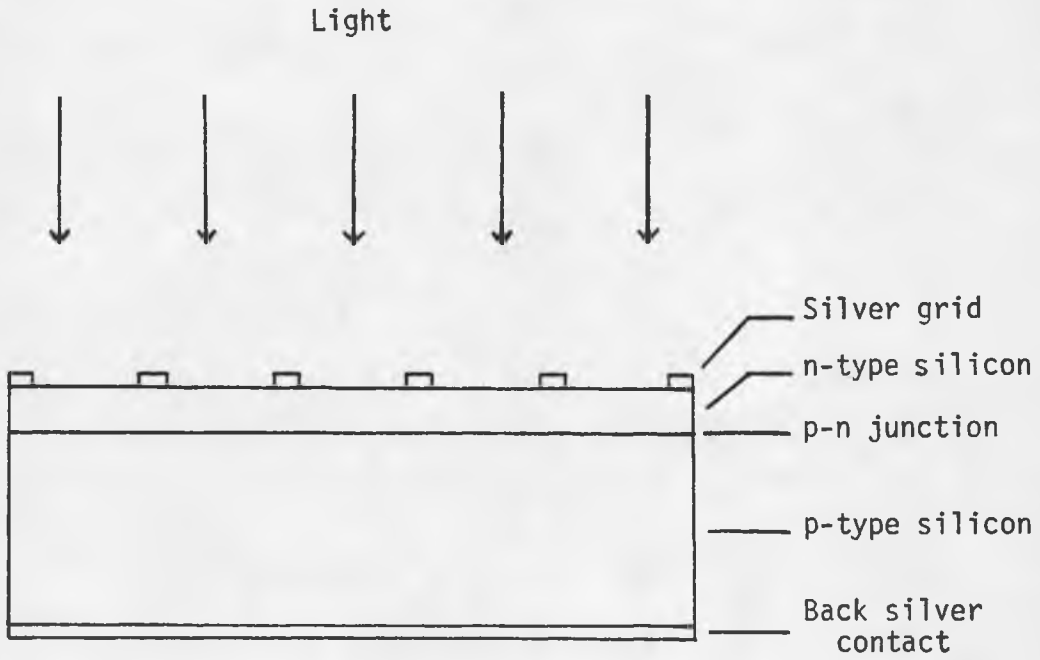

Figure 1. Cross sectional diagram of a silicon solar cell.

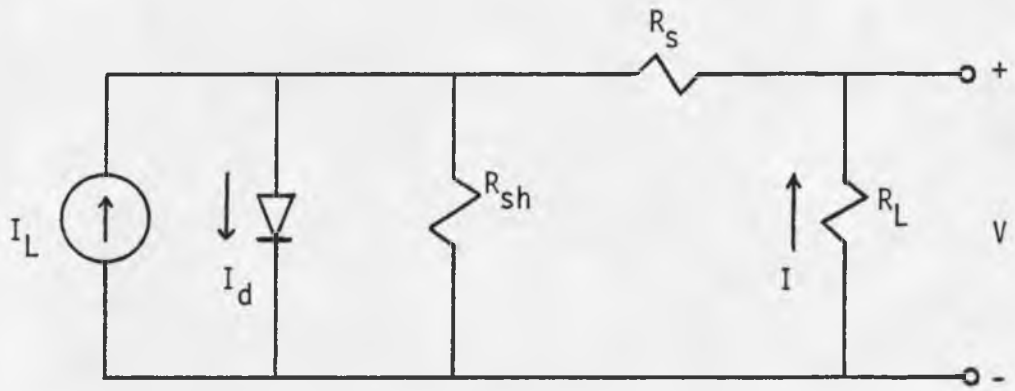

Figure 2. An equivalent electrical circuit of a solar cell.

where $B = \frac{q}{KT}$

q = electron charge

K = the Boltzman constant

T = cell temperature (^{o}K)

I_s = reverse saturation current

A well made solar cell typically has a very low series resistance and a very high shunt resistance. In such cases the approximations $R_{sh} \rightarrow \infty$ and $R_s \rightarrow 0$ can be made which reduces equation (1) to equation (2). It should be noted that the dark current I_d through the diode is $I_s \left\{ \exp(BV)-1 \right\}$. The reverse saturation current I_s for 2cm x 2cm 40X Solarex cells is 2.43×10^{-12} amperes (Backus and associates 1978, p. 2.14a).

$$I = I_s \left\{ \exp(BV) - 1 \right\} - I_L \qquad (2)$$

Photovoltaic solar cells are commonly described through three parameters, the short circuit current I_{sc}, the open circuit voltage V_{oc}, and the curve fill factor CFF, which are described by equations (3), (4), and (5).

$$I_{sc} = -I_L \qquad (3)$$

$$V_{oc} = \frac{KT}{q} \ln \frac{I_L + I_s}{I_s} \qquad (4)$$

$$CFF = \frac{V_m I_m}{V_{oc} I_{sc}} \qquad (5)$$

Equations (3) and (4) are derived directly from equation (2). The curve fill factor is determined graphically from the characteristic I-V curve of a cell as illustrated in Figure 3. V_m and I_m are the voltage and

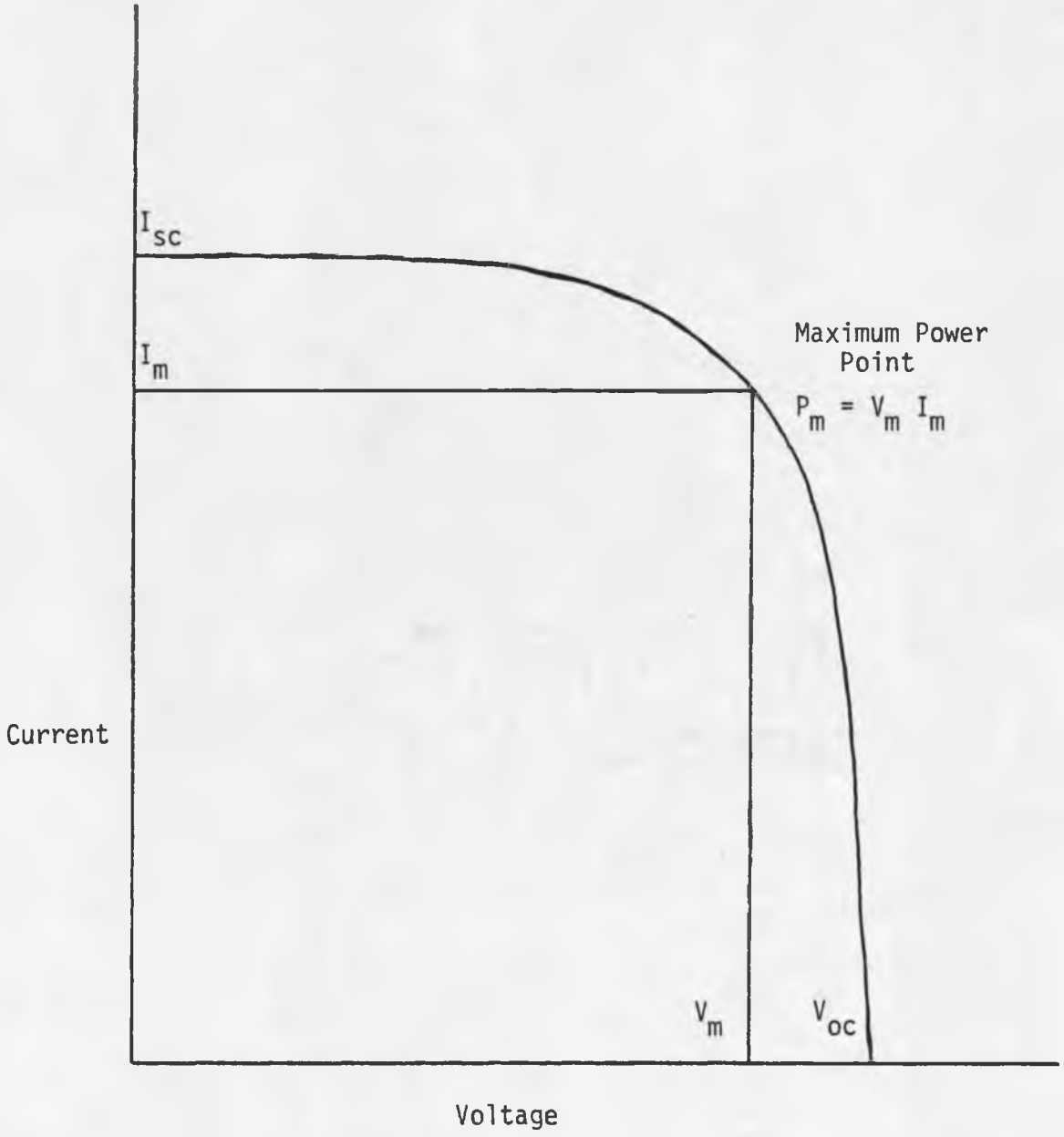

Figure 3. A typical I-V curve for a solar cell.

current respectively at the maximum power point P_m located near the knee of the curve. The more the I-V curve resembles a rectangular shape the higher the cell's efficiency and CFF will be.

The equivalent circuit and equations discussed above can be used to describe the electrical output of a solar cell. However, they can also be used to describe a complete system of cells connected together as in a photovoltaic concentrator. The I-V curve of a system of solar cells will be similar to the I-V curve of a single cell except that the current and voltage values will be larger. The short circuit current, open circuit voltage, and curve fill factor for a photovoltaic system are all determined from the I-V curve as in the case of a single cell.

Concentrator Components Supplied by Arizona Scientific Research

Arizona Scientific Research (ASR) provided the optical modules and heat sinks needed to construct six solar concentrators. Each heat sink or receiver was a hexagonal prism machined on the surface of a metal pipe with the hexagonal shape around the circumference. The receiver holds 18 2cm x 2cm, 40X solar cells. Three cells were mounted on each of the six faces of the receiver which were 2.2 cm wide. Three receivers were actively cooled as shown in Figure 4. The three other receivers had a similar design but used heat pipes to reject heat out the bottom end. In one case the bottom end of the heat pipe was passively cooled with air fins. In the two other cases the heat pipes were cooled by water circulating in tubes surrounding the bottom ends of the heat pipes.

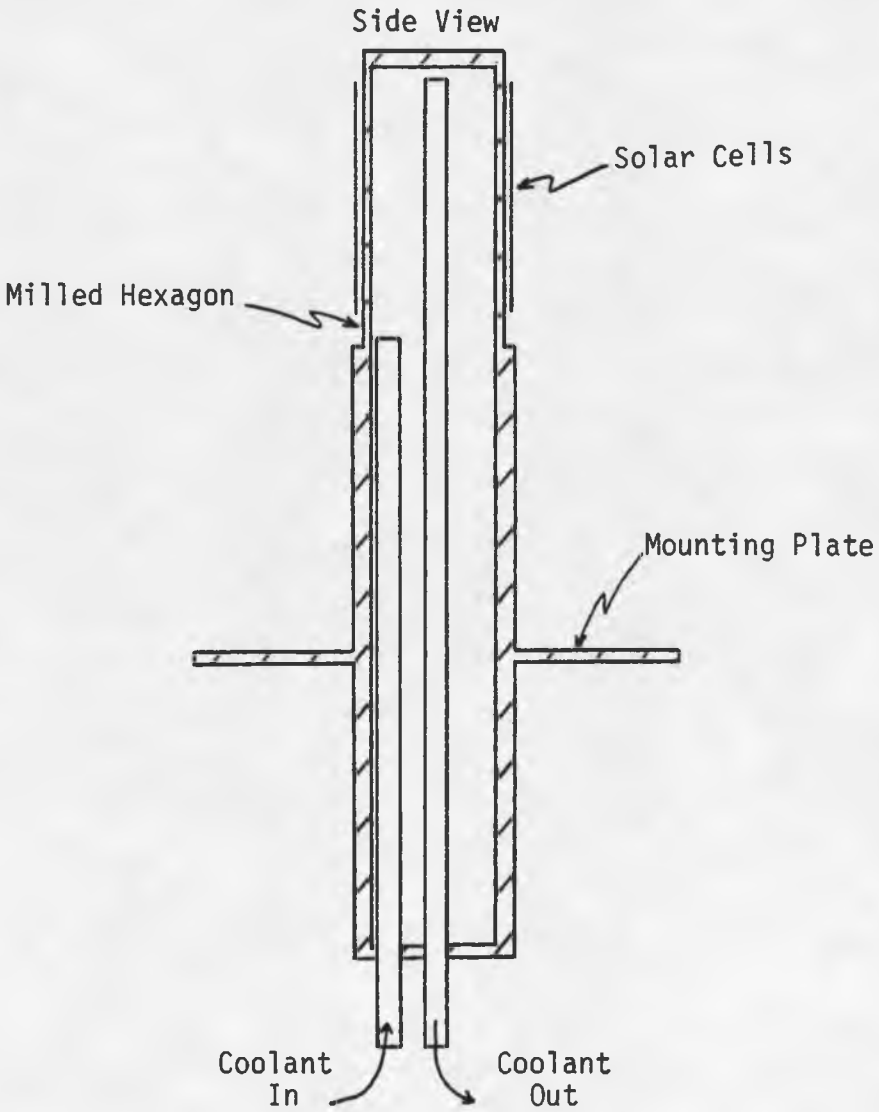

Figure 4. An actively cooled receiver.

Sunlight was focused on the central hexagonal receivers by the ASR optical modules. Five of the optical modules were made from plexiglas and one was made from ABS plastic. One module had evaporated silver as the reflective surface. Another used copper. The remaining four optical modules had aluminum deposited as the reflective surface.

Each optical module had five conical sections that focused sunlight on the receiver. Figure 5 depicts an optical module together with an actively cooled receiver. Each conical section overlaps a parallel section of sunlight on the receiver resulting in a small intensity variation along the receiver. The modules have been designed so that the average concentration ratio is 40X.

Research was carried out in several areas before solar cells were mounted in a concentrator. In order to keep the electrical output as high as possible, it was important to keep the solar cells relatively cool. The cells could not be electrically shorted to the metal receiver. Thus, it was necessary to find a mounting procedure which conducts heat efficiently from the cells to the receiver yet keeps the cells electrically insulated from the receiver. Before the solar cells were attached to the receivers, electrical connections were made to the back sides of the cells. An electrically conducting substrate on which cells could be mounted was selected for this purpose. Solar cells under very intense light generate relatively large currents. Therefore, it was very important that all electrical interconnections add little or no series resistance in order to keep the module performance from degrading. All these problems were thoroughly investigated.

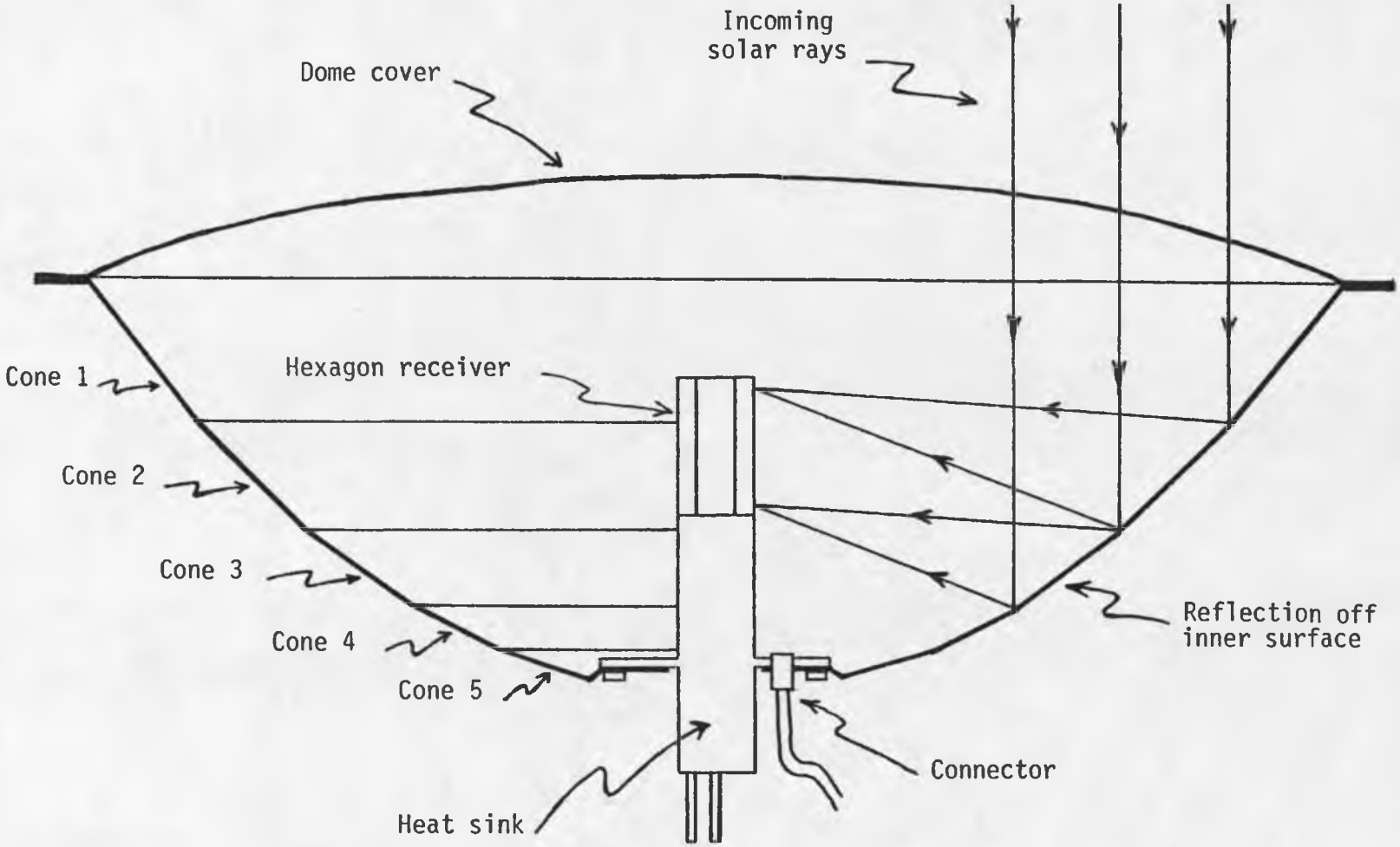

Figure 5. Optical module with actively cooled receiver.

Finally, the performance of the completed module was evaluated. The electrical performance of each receiver, the efficiency of each method of cooling, and the optical efficiency of each optical module was investigated. An analysis of the module's overall electrical efficiency was conducted to determine where improvements could be made.

CHAPTER II

MOUNTING CELLS ONTO MOLYBDENUM

Before the solar cells were mounted onto heat sinks, a means was devised by which the electric current could be collected from the back side of the cell. Experiments led to a technique for mounting the cells onto flat pieces of molybdenum. Electrical leads could then be soldered onto the molybdenum to make contact with the back side of the cell.

Substrate Selection

When a light concentration of 40 suns was focused onto solar cells the surface temperature of the cells increased significantly even when active cooling was used. Consequently, the cells as well as the substrate on which they are mounted will go through many cycles of expansion and contraction. In order to minimize the stress on the cells and reduce the possibility of fracturing or contact lifting, a substrate was chosen which has a coefficient of expansion close to that of silicon. The CRC Handbook of Chemistry and Physics (1974-1975, p. D-152) shows that silicon has a coefficient of expansion of 3 $\mu m/m^{o}C$. Molybdenum was chosen as the substrate material since its coefficient of expansion of 5 $\mu m/m^{o}C$ is closer to that of silicon than any other metal.

The solar cells were mounted onto a molybdenum substrate for the purpose of making electrical contact with the back side of the cells. In order to insure that the cells were adequately supported, the molybdenum substrate covered the complete back side of the cells. This also made

matters easier when the cell-substrate combinations were mounted onto the molybdenum substrates using solder to ensure good thermal contact and to minimize the series resistance, R_s.

Solarex solar cells, 2cm x 2cm, were used in this project. A diagram of the cell is found in Figure 6. To accommodate the cells the molybdenum was cut into 2.0cm x 2.2cm pieces. The extra 0.2 cm in one dimension was for the edge which was bent up for the electrical connection to the back side of the cell. Molybdenum thicknesses of 0.13 mm, 0.25 mm, and 0.38 mm were cut and prepared for cell mounting. It soon became evident that the 0.13 mm molybdenum was very flimsy and difficult to work with. No such problems were encountered in preparing the other two thicknesses. However, for the sake of maximum heat transfer the thinner 0.25 mm molybdenum was chosen as the substrate thickness.

Electroplating and Cell Mounting

A coating of copper was electroplated to the bottom and top contact areas of the solar cells. This was done to prevent the silver on the cell contacts from alloying with the solder when the molybdenum and top electrical connections were soldered to the cells. A solution of 188g/ℓ copper sulfate ($CuSO_4 \cdot 5H_2O$) and 74g/ℓ sulfuric acid (H_2SO_4) was used in the electroplating process (Gray 1953, p. 235). The top contact pads were plated for about 45 seconds using 50 mA of current. The back side of each cell was plated for two minutes using 175 mA of current. After plating, a thin layer of solder was coated onto the back side of the cell using a soldering iron.

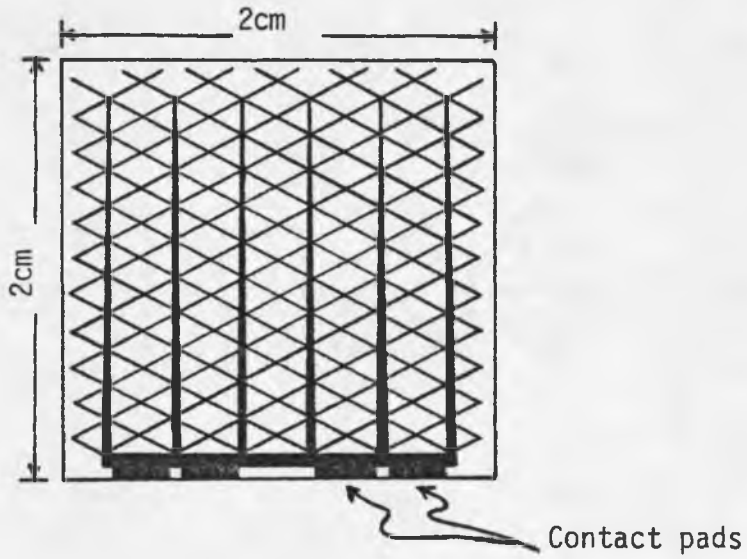

Figure 6. Solarex solar cell.

The solar cells were soldered onto the molybdenum substrates. However, solder will not adhere to molybdenum so it also needed to be plated first. Initially copper was plated onto the molybdenum but the copper layer would not adhere well to the molybdenum. A nickel plate using a solution of 300g/ℓ nickel sulfate ($NiSO_4 \cdot 7H_2O$), 60g/ℓ nickel chloride ($NiCl_2 \cdot 6H_2O$), and 38g/ℓ boric acid (H_3BO_3) was tried next (Gray 1953, p. 303). This electroplating was carried out with only limited success. The nickel plate adhered better than the copper but it would also peel off occasionally. In order to give the plated metal a better surface on which to adhere, the molybdenum metal, which previously had been very smooth, was given a thorough sandpaper rub. Experiments were then performed plating both copper and nickel onto the sanded molybdenum. Both appeared to plate well onto the molybdenum so tests were performed to see which plate had the stronger adhesion. It was determined that the nickel plate adhered better so nickel plated molybdenum was used from that point on.

To prepare the molybdenum for cell mounting it was first cut into 2.0cm x 2.2cm pieces. The pieces were then sanded and the one edge was bent up for the back electrical connection. In order to ensure a clean surface before plating, the molybdenum pieces were dipped in a solution of four parts H_2SO_4 and one part H_2O_2 at a temperature of 90^oC for 10 seconds. After an adequate rinse, nickel was plated onto the molybdenum using a current of 200 mA for two minutes. A thin coating of solder was then applied to the molybdenum using a hot plate and soldering iron. The back of the cell and the molybdenum substrate were put in contact and heated on a hot plate to melt the solder and make

the bond between them. When the solder melted, the excess solder was squeezed out the sides.

After the above procedure was completed the cells were ready to be individually electrically tested. The cell-substrate combinations were also ready to be mounted onto heat sinks. However, it was necessary first to determine a good heat conducting adhesive and a proper mounting procedure. This is covered in Chapter IV.

CHAPTER III

ELECTRICALLY TESTING INDIVIDUAL CELLS

Before the solar cells were mounted in modules, electrical tests were performed on all the cells individually. The data were collected in the form of I-V curves from which all necessary information could be extracted. These preliminary tests are important for several reasons. If any cells are defective, they must be detected before being mounted in a module. The efficiency of each cell was determined so cells with similar efficiencies could be put in the same module. This was important because if cells with a variety of different efficiencies were in the same module, the overall performance of the module would only be as good as the worst cell.

Setup for Making I-V Curves

An indoor solar cell tester using quartz iodine electric lamps was designed to give consistent results as well as to make the test procedure simple and easy. General Electric ENH 250 watt projector lamps were used as the light sources in the solar simulator. A single lamp was placed at 40 cm from the target area to simulate one sun (1 sun AMI = 100mW/cm^2). Five other lamps were each placed 13 cm from the target area, each providing the equivalent intensity of 10 suns. Thus, an intensity of 50 suns could be focused on the target area if so desired. Frequent checks, using a standard cell, were made and the lamp positions were adjusted accordingly to ensure that the correct intensity was maintained. The target area consisted of an aluminum

heat sink through which water was circulated for cooling. Figure 7 shows a cell-substrate combination mounted on the aluminum heat sink ready for an electrical test.

A diagram of the electrical test apparatus is shown in Figure 8. The resistor shown in the circuit was a precision 0.01Ω resistor. Current was found by measuring the voltage drop across this resistor. The voltage across the cell would be V-IR where V was the voltage of the power supply. The product IR was very small with respect to V. Thus the cell voltage was effectively the same as V. As V, the cell voltage, was varied the cell current I was forced to change along the characteristic I-V curve. The cell voltage and current were measured simultaneously by the X-Y recorded which made the I-V plot.

Calibrating the Standard Cell

Whenever data was being collected, the exact intensity of light was determined through the use of a standard cell. In order to calibrate this cell exactly, its short circuit current readings were compared with the accurate solar insulation measurements taken at the Atmospheric Sciences' weather station. The weather station data, standard cell data, and conversion factors are all recorded in Table I.

The average conversion factor is 113mA/1 sun or $113mA \cdot cm^2/100mW$. Since the short circuit current I_{sc} of the standard cell is proportional to solar intensity, the exact solar intensity can be found using equation (6).

$$\text{Solar Intensity } (mW/cm^2) = \frac{I_{sc}\ (mA)}{(113mA \cdot cm^2/100mW)} \qquad (6)$$

Figure 7. A solar cell mounted for an electrical test.

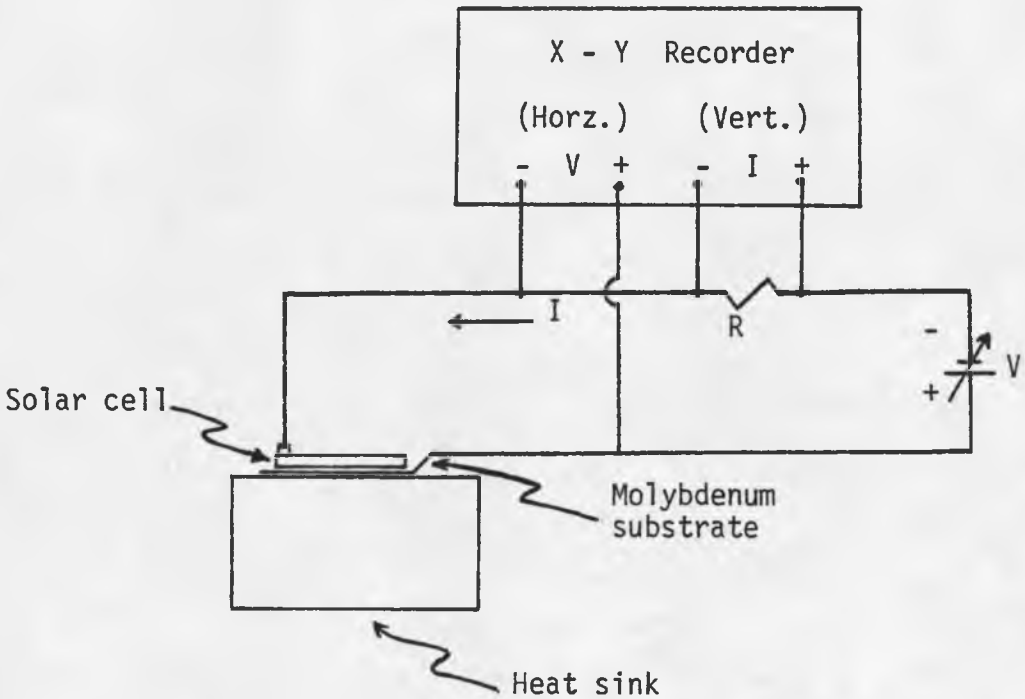

Figure 8. Single cell electrical test apparatus.

Table I. Standard cell calibration data

Date	Time	Solar insolation	Standard cell reading	Conversion factor
1/08/79	11:30 am	92.0 mW/cm^2	102 mA	110.9 mA/1 sun
1/08/79	1:50 pm	92.1	105	114.0
1/08/79	2:20 pm	90.1	101	112.1
1/08/79	2:45 pm	89.5	100	111.7
1/30/79	2:00 pm	101.2	113	111.6
1/30/79	2:40 pm	98.8	113	114.4
2/02/79	12:10 pm	98.8	112	113.3
2/06/79	3:00 pm	92.8	105	113.1

Individual Cell Tests

According to specifications, the 2cm x 2cm cells purchased from Solarex should produce an electrical output of 2 watts at 25°C under a light intensity of 40 suns. Thus, a typical cell should have an efficiency of 12.5%. Each cell was tested to make sure that none were defective and also to find the exact efficiency of each.

The first step in cell testing was to look for defective cells by measuring the short circuit current of each under one sun. This was done before any soldering or connections were made to the cells. Electrical contacts were made through the aluminum heat sink on the bottom and point probes on the top. As expected, some cells were better than others but none proved to be defective. The average short circuit current under an intensity of one sun was 92 mA. In

making one sun I-V curves, a problem was encountered with an abnormally high series resistance causing a low curve fill factor. This was due to contact resistance between the back side of the cell and the aluminum heat sink. A drop of water between the cell and the heat sink corrected this problem. A typical I-V curve for a Solarex cell using an intensity of one sun is shown in Figure 9.

The next step was to mount the cells on the molybdenum substrates and perform electrical tests with high concentrations of light. In order to be sure that the process of soldering the cells to the molybdenum did not damage the cells or degrade their performance, only a few cells were initially mounted. I-V curves of these cells were compared with curves taken before mounting. As Figure 10 shows, there is only a small difference between the two cases with the mounted cell having a slightly better performance. The slight improvement is due to a further reduction in series resistance. Contact to the back of the cell was now made by a direct connection to the molybdenum substrate instead of through the aluminum heat sink.

Every cell was tested in the solar simulator using light intensities of 10, 20, 30, 40, and 50 suns. A typical representation of the resulting curves is seen in Figure 11. The average efficiency η of the cells at 40 suns was 11.0%. The average cell temperature at 40 suns was determined to be 45^{o}C. If the peak power voltage V_m is corrected to 25^{o}C using the factor 2mV/^{o}C, the average efficiency is 11.8%. This compares with 12.5% which is what the Solarex specifications say the efficiency should be at 25^{o}C.

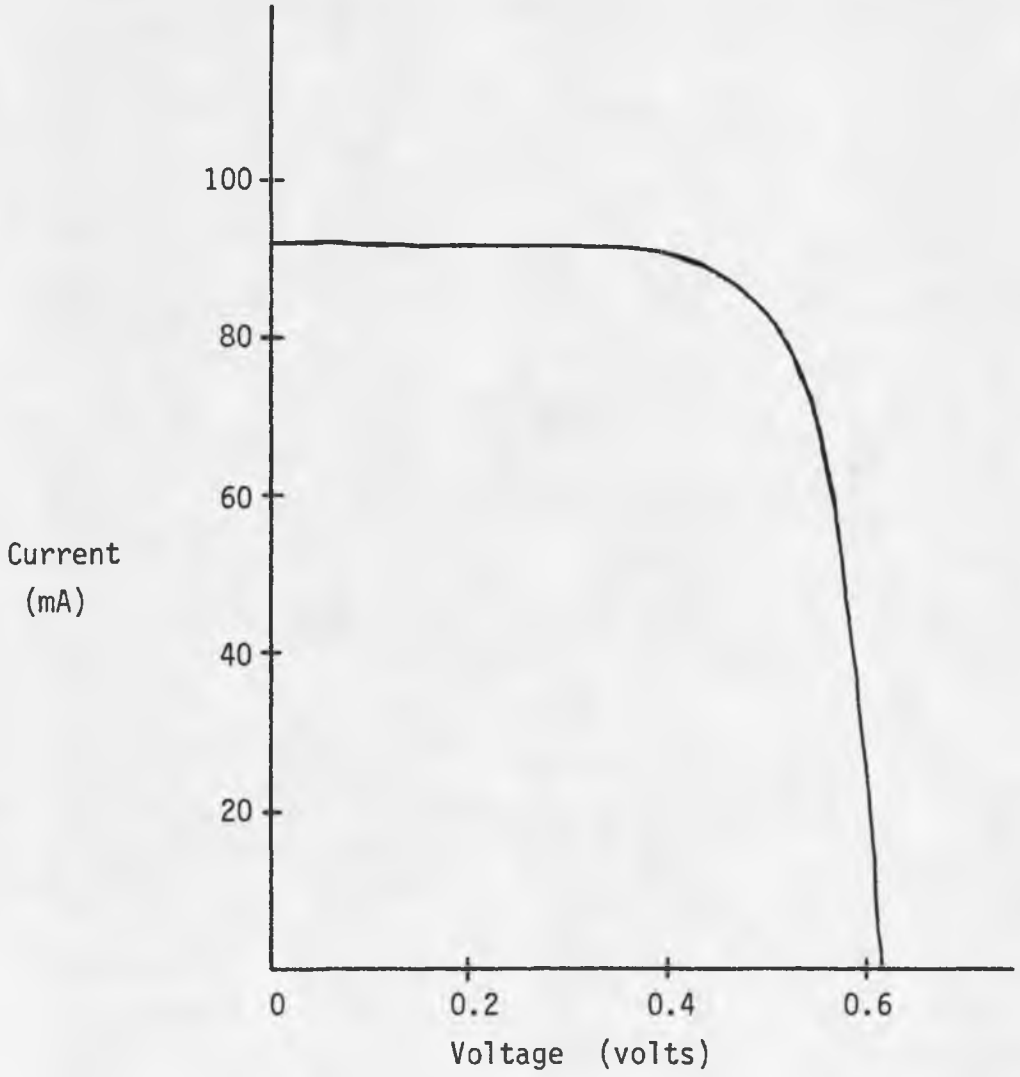

Figure 9. Solarex cell I-V curve at one sun.

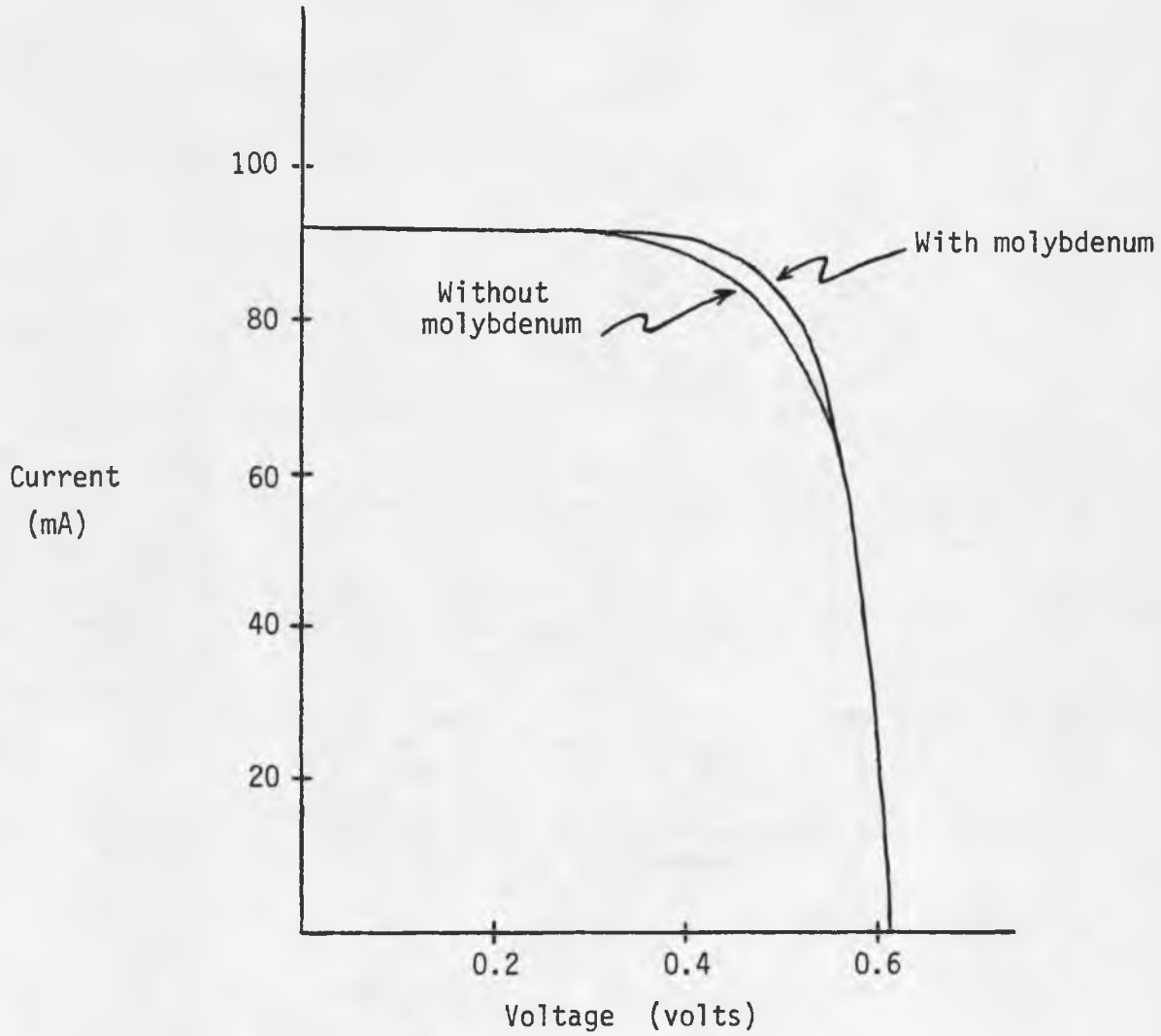

Figure 10. I-V curves at one sun before and after molybdenum mounting.

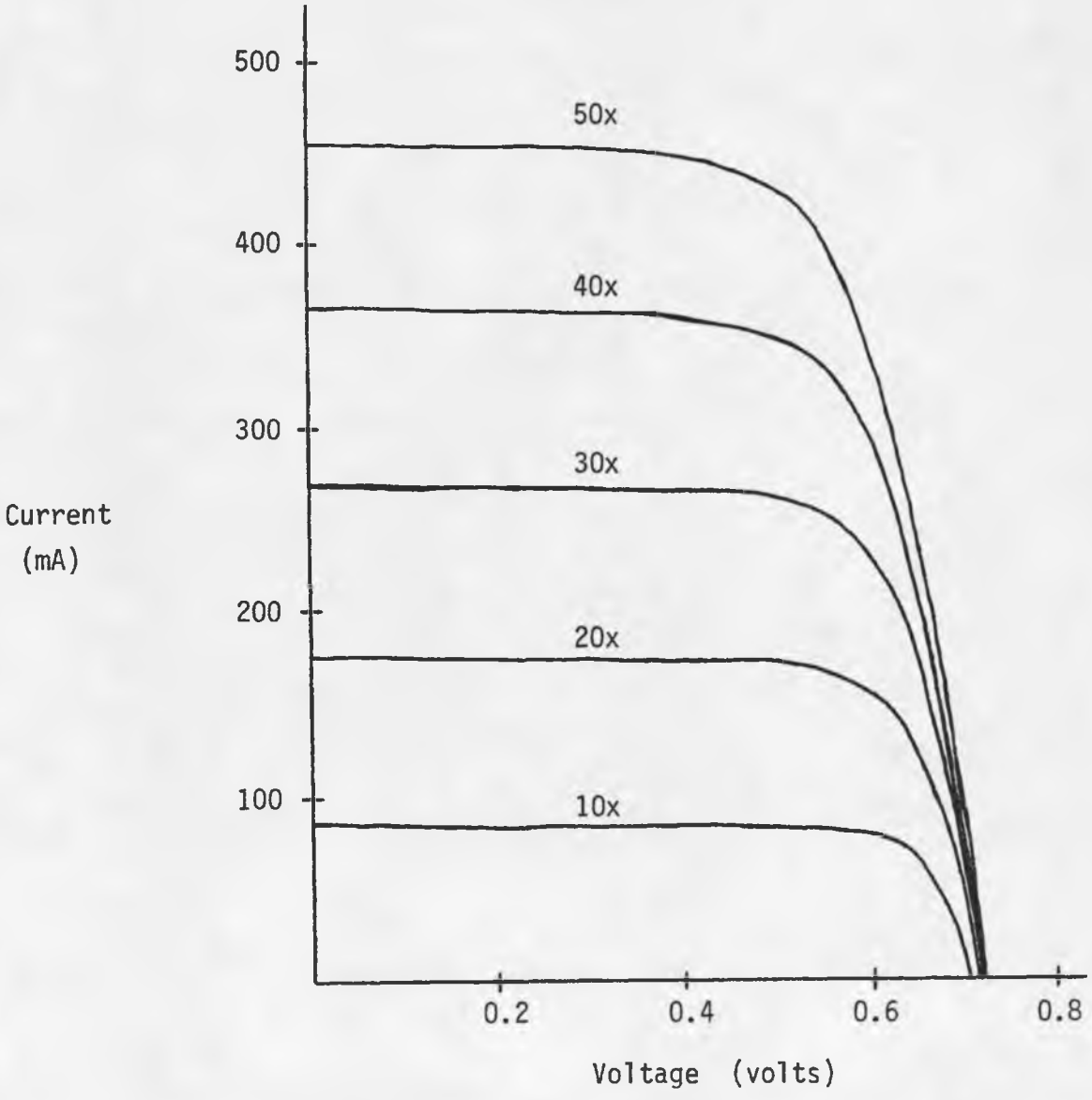

Figure 11. I-V curves for 10-50 suns of intensity.

Cell Efficiency Versus Light Intensity

The efficiency of a cell will vary with light intensity. Using the curves of Figure 11, the efficiencies were calculated for each light intensity. The cell temperature was monitored while the curves were traced. The calculated efficiencies were compared to the efficiencies of Solarex 40X cells calculated by the School of Engineering at Arizona State University (ASU) (Backus and associates 1978, p. 2-31). In order to be able to compare data, all values were corrected to 25°C. Power and efficiency data, before and after being corrected to 25°C, are given in Table II.

Table II. Cell peak power and efficiency versus light intensity

Light intensity	Cell temp.	P_m	η	P_m corrected to 25°C	η corrected to 25°C
50 suns	50°C	2.08W	10.4%	2.28W	11.4%
40	45	1.74	10.9	1.86	11.7
30	40	1.36	11.4	1.44	12.0
20	35	0.92	11.6	0.96	12.0
10	30	0.45	11.2	0.46	11.4

The corrected efficiencies are compared with ASU's data using curves which plot efficiency versus solar intensity. Both curves are shown in Figure 12. The cells used in this project have slightly better efficiencies than those used by ASU. The reason is probably because the cells used for this project are a year newer. Solarex has probably made improvements in the performance of the more recent cells.

All curves temperature corrected to 25°C

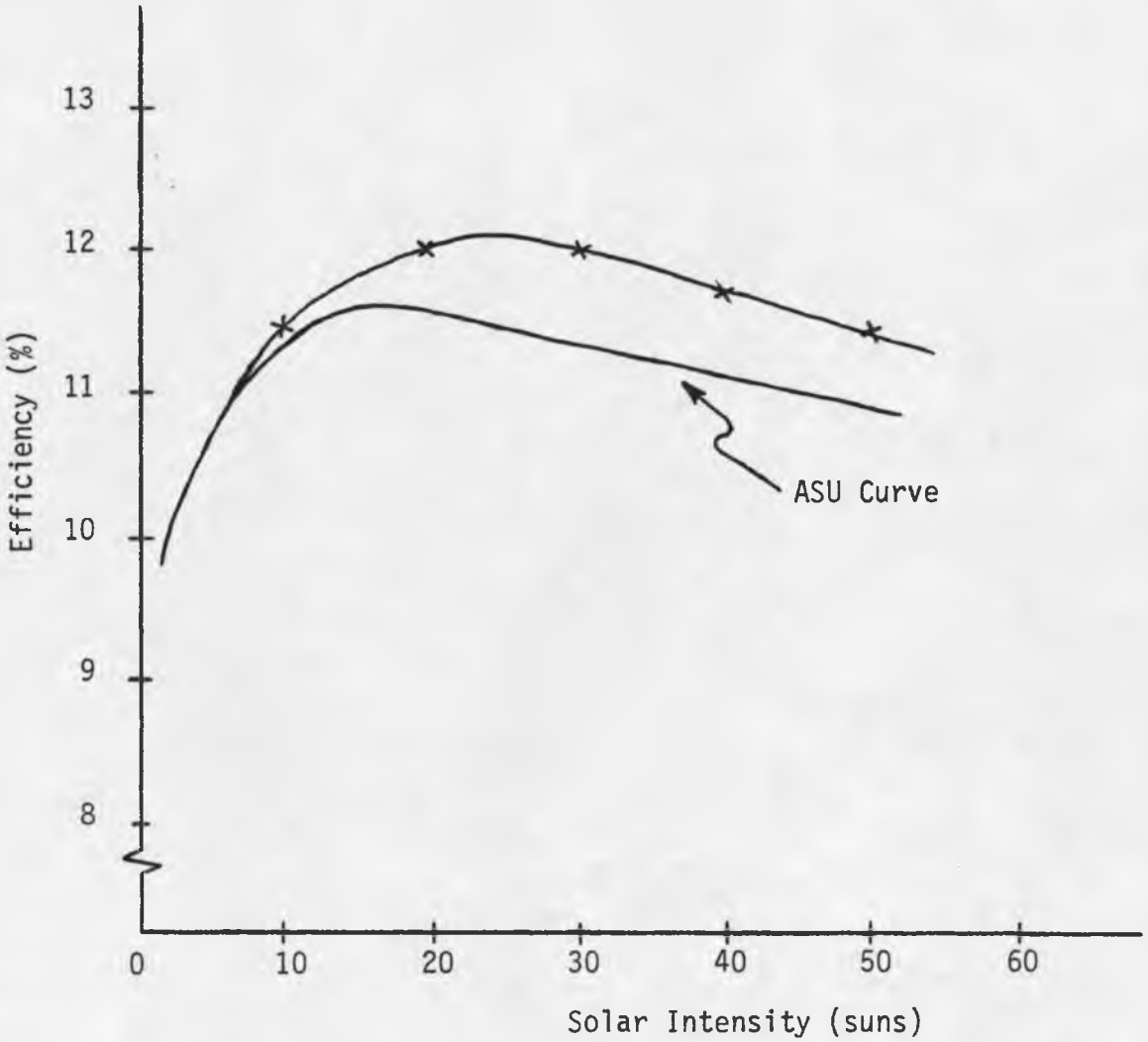

Figure 12. Laboratory and ASU curves comparing efficiency and light intensity.

CHAPTER IV

PROCEDURE FOR MOUNTING CELLS ONTO HEAT SINKS

Before the cells could be mounted in a concentrator, a practical means of mounting the cell-molybdenum combination onto a heat sink needed to be devised. This technique must use an adhesive which provides good heat conduction between the molybdenum substrate and heat sink while keeping them electrically insulated from each other.

Procedure for Attaching Thermocouples

In order to determine which adhesives provided good or poor heat conduction, temperatures had to be monitored throughout all tests. All temperature measurements were made with the use of copper-constantan thermocouples. Figure 13 shows where the thermocouples (TC) were placed. A small trench was cut in the top of the heat sink. TC1 was laid in this trench to monitor the temperature of the heat sink just below the adhesive. TC's 2, 3, and 4 were mounted in various places on the cell or molybdenum substrate. Before measurements could be made, a method of attaching thermocouples was needed which would give accurate results.

Tests showed that a good thermal contact was necessary between the thermocouple and the material whose temperature was to be measured. In the following experiment, three cases were tested. In case 1 TC3 was attached firmly to the top of the cell with silver paint, a paint which contains a large proportion of powdered silver. In case 2 TC3 was laid on top of the cell and no material was used to enhance the

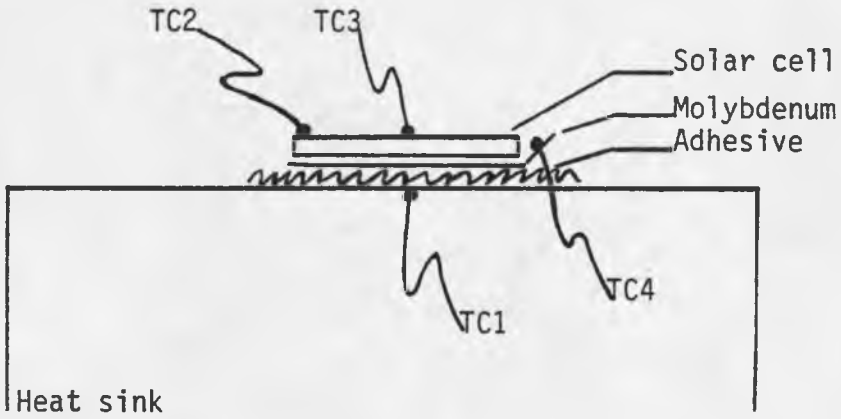

Figure 13. Thermocouple locations for temperature test measurements.

thermal contact between the thermocouple and the cell. In case 3, the thermocouple was raised slightly to put it just out of contact with the cell. The data summarized in Table III were all taken using a light intensity of 40 suns.

Table III. Thermocouple measurements with varying degrees of thermal contact

	TC1	TC3	ΔT_{31}
Case 1	26°C	44°C	18°C
Case 2	29	68	39
Case 3	28	71	48

If the thermocouple TC3 does not have good thermal contact with the cell, as in case 2 and case 3, temperature measurements are abnormally high. The small thermocouple wires are in the path of the light. If there is not a good thermal contact between the end of the thermocouple and the cell, excess heat builds up in the wires and an erroneously high temperature is read. On the other hand, if a good thermal contact exists, heat can flow freely between the cell and the thermocouple and TC3 will be at the same temperature as the cell.

A test was devised to study several compounds which could be used to attach thermocouples. These included silver paint, beryllium oxide paste, and silicone grease. Everything was removed from the top of the water cooled heat sink except TC1 which remained in the

narrow trench. TC3 was attached to the heat sink near TC1 using one of the three compounds. Temperature measurements were taken for each compound at 40 suns. Table IV summarizes the results.

Table IV. A comparison of thermocouple attachment compounds

Compound	TC1	TC3	ΔT_{31}
Silver paint	26°C	27°C	1°C
Beryllium oxide paste	25	30	5
Silicone grease	26	36	10

TC1 and TC3 are both measuring the temperature of the aluminum heat sink so they should be reading the same temperature. Silver paint gave the best correlation between TC1 and TC3. It is apparent that attaching thermocouples with silver paint gives the most accurate results.

One other possibility existed for attaching thermocoples. On solderable surfaces thermocouples could be soldered into position. As one might expect temperature comparisons between thermocouples attached with solder and silver paint showed a close correlation between the two cases. Either method of attachment could be used to obtain accurate temperature measurements.

Heat Conducting Adhesive Selection

Various electrically insulating adhesives were tested for thermal conductivity. A good heat conductor, through which heat passes,

will have a relatively small temperature gradient across it. In the tests run, thermocouples were set up as shown in Figure 13. The thermocouples were attached using silver paint. Temperature differences between the top of the cell and the bottom of the adhesive were measured. This includes the temperature differences across the cell and molybdenum as well as the temperature difference across the adhesive. However, due to the high thermal conductivity of silicon and molybdenum, most of the measured temperature drop will occur across the adhesive.

The two most promising adhesives were a silicone rubber sealant and RTV-560. In all cases, an adhesive thickness of 0.1 mm was used. Using 0.05 mm thick tape as a guide, 0.05 mm of adhesive was put on the heat sink and allowed to dry. Then 0.05 mm of adhesive was applied to the back side of the molybdenum substrate. The cell-substrate combination was immediately placed on the heat sink where the adhesive had previously been applied. Under pressure, the adhesive was allowed to dry forming the bond between the molybdenum and the heat sink.

The silicone rubber sealant was used with varying concentrations of powdered silicon mixed in to increase heat conduction. Volume ratios of 0:1, 1:1, and 2:1 silicon powder to silicone rubber were used to show the effects of silicon in silicone rubber. Table V summarizes the temperatures which were observed under a light intensity of 40 suns.

The higher concentrations of silicon powder will indeed make the compound more heat conductive. However, there are limitations. If the silicon powder concentration is too high, the mixture is very dry and difficult to work with. The compound also does not "wet" the surfaces as well which begins to reduce heat conduction. As a compromise,

Table V. Temperature results with the silicone rubber adhesive

Ratio silicon to silicone rubber	Heat sink temp.	Cell temp.	Temperature difference
0:1	21°C	42°C	21°C
1:1	26	43	17
2:1	26	42	16

it is best to use the silicon powder ratio of 1:1.

A test was run comparing the heat conduction properties of RTV-560 and silicone rubber. Both were tested using a 1:1 ratio by volume of silicon powder to adhesive. While the silicone rubber mixture had a temperature difference between the cell and heat sink of about 17°C, the RTV-560 mixture had a temperature difference of 14°C. RTV-560 will conduct heat slightly better than silicone rubber. However, for several reasons silicone rubber was selected over RTV-560. RTV-560 adhered very poorly to the smooth metal surfaces which were used. No such problems were encountered with silicone rubber. RTV-560 was also more difficult to work with because it was necessary to mix in a catalyst for curing. In light of this as well as the fact that RTV-560 is only a slightly better thermal conductor, silicone rubber was selected as the adhesive to be used.

Another test was conducted using silicone rubber. This time copper powder, instead of silicon powder, was mixed with the silicone rubber in a 1:1 ratio. At 40 suns, this gave a cell-to-heat sink temperature difference of 13°C. This was an improvement but the silicone

rubber became electrically conductive due to the presence of copper powder. Reducing the copper concentration enough to make sure the compound was no longer electrically conductive resulted in a thermal conduction that was no better than the mixture of silicone rubber and silicon powder.

A cell-substrate combination was mounted onto a small copper plate using the adhesive mixture of silicone rubber and silicon powder. The copper plate was then cycled daily on and off of a hot plate maintained at 200°C. The cycling was continued over a period of six weeks in order to see if silicon rubber could withstand high temperatures over long periods of time without deteriorating. Throughout the cycling, there was no deterioration in the silicone rubber.

Temperature Measurements of All Mounting Components

A cell-molybdenum combination was mounted on the water cooled heat sink using silicone rubber and silicon powder in a 1:1 ratio. Under various light intensities, the temperatures of several locations were monitored. As shown in Figure 13, TC1 was used to measure the temperature of the heat sink just below the silicon rubber. TC2 was soldered to the top contact pad of the solar cell. Using silver paint, TC3 was attached to the top of the cell near the center. TC4 was soldered onto the molybdenum edge where the cell interconnections would be placed. The temperatures were recorded using light intensities of 10, 20, 30, and 40 suns. The results are summarized in Table VI.

The temperature differences between the top of the cell and the heat sink were what would have been expected from previous experimental results. One would expect the temperature of the top contact pad to be close to that of the cell surface. However the contact pad temperatures

Table VI. Temperature measurements of a mounted solar cell

Light intensity	Heat sink	Contact pad	Cell surface	Molybdenum edge	Cell-to-heat sink ΔT
10 suns	26°C	33°C	33°C	40°C	7°C
20	27	38	39	51	12
30	27	46	41	63	14
40	28	51	45	76	17

were slightly higher. The temperatures of the molybdenum were much higher than the cell temperatures. This would be expected because the molybdenum edge had been bent up away from the heat sink allowing this area to get relatively warm.

At this point, all preliminary tests and experiments necessary before module assembly had been completed. A mounting procedure was developed that would keep the cell temperature as low as possible and minimize any stress and strain on the cell due to expansion and contraction. In determing the mounting procedure, accommodations were made for easy cell interconnections. The methods developed to plot cell I-V curves and make thermal measurements on single cells were also used in gathering data from completed modules.

CHAPTER V

MODULE DATA

Using the techniques developed in previous experiments, the modules were assembled into finished products. Several characteristics of the completed modules were investigated. Electrical measurements were used to test the quality and performance of each receiver and optical module. The temperatures of various locations on each receiver were monitored to see if the various cooling methods were removing heat adequately. Finally, the optics of the reflector were analyzed.

Module Assembly

Six heat sinks or receivers were constructed. Each had six machined surfaces in a hexagonal shape. Each surface was designed to accommodate three cells so eighteen solar cells mounted on molybdenum substrates were mounted on each receiver. Each of the flat surfaces on the receiver was coated with 0.05 mm of silicone rubber and silicon powder mixed in a 1:1 ratio. After curing, another 0.05 mm of the adhesive was applied to the bottom side of the molybdenum substrate. While the adhesive was still wet, the cell-molybdenum combination was pressed onto the receiver. The three cells of each face were mounted at the same time. They were mounted as close together as possible to reduce optical losses. However, a small distance had to be maintained between them to keep neighboring cells or molybdenum substrates from contacting each other. The resistance was measured between every molybdenum substrate and the receiver on which it was mounted. This was done to be sure they were electrically insulated.

Three methods of receiver cooling were employed. Receiver #1. #2, and #3 were all constructed in a similar manner. As shown in Figure 4, these actively cooled receivers were hollowed out inside. Two metal tubes were inserted through the bottom to provide an inlet and outlet for water. Receivers #4 and #5 were both constructed from aluminum pipes. The upper ends of each were left open to allow the insertion of a heat pipe which fit snugly down the center of each receiver. The lower end of the heat pipe was surrounded snugly by another aluminum pipe. It was cooled by a ¼" aluminum tube wrapped around and welded to the outside of the pipe. A flow of water was provided through the ¼" tube. Figure 14 depicts a receiver cooled with a heat pipe. Receiver #6 was very similar to #4 and #5. However, in this case the lower end of the heat pipe was cooled passively by heat fins made of cast aluminum.

Once mounted on the receivers, the cells were interconnected in one of two possible ways. Putting all eighteen cells in series, denoted as 1P x 18S, allowed the highest possible voltage at the lowest current. Under 40 suns a single cell should produce about 0.55 volts and 3.2 amperes at the maximum power point. This would yield 10 volts at 3.2 amperes for the module. Power losses due to series resistance would be smaller with the 1P x 18S wiring because of the small current. However, if all eighteen cells are not uniformly illuminated, the module current is limited by the current generation of the cell with the least illumination. Since non-uniform light distribution was expected along the vertical axis of the receivers, a second connection configuration was also used to lessen some of the problems associated with non-uniform light distribution. The three cells on each face were wired in parallel.

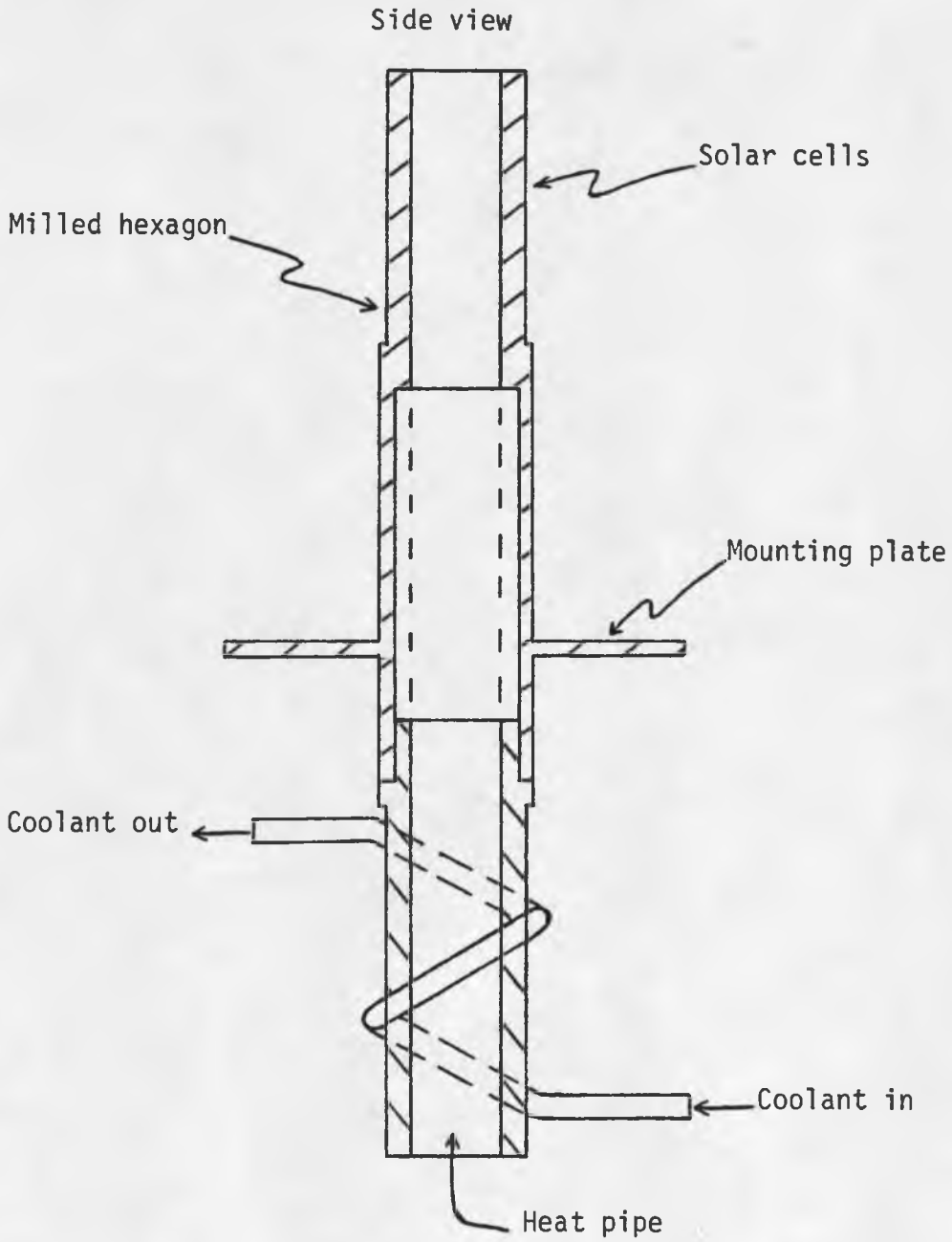

Figure 14. Receiver cooled with heat pipe.

The six faces were then wired in series. Wiring in this fashion is denoted as a 3P x 6S configuration. The cells on receivers #2, #4, #5, and #6 were connected in this manner. The cells on receiver #1 were connected in the 1P x 18S configuration. The wiring on receiver #3 was changed once so that both options could be tested using the same cells.

The interconnections between cells were made with copper braid. The flexibility of braid was desirable because it made it easier to connect the cells together and would cause less strain on the cell contacts after the connections had been soldered. A braid with 64 strands of 0.075 mm diameter copper wire was used. Even with the maximum possible current in a 3P x 6S configuration, only 3% of the electrical output would be lost due to wiring series resistance. In the 1P x 18S configuration, the wiring losses would be a maximum of 1%.

Cells of similar efficiencies were mounted on each receiver. The average cell efficiency as well as the other characteristics of each receiver are summarized in Table VII.

Six copper-constantan thermocouples were attached with silver paint to various points on each receiver. Temperatures were monitored for several reasons. The efficiency of each method of receiver cooling was to be determined. The actual cell temperatures were also monitored to determine how much the module output was degraded due to cell heating. Thermocouple wires were fed through holes in a plastic plug at the base of the receiver. The wires ended on terminal boards attached to the receiver base.

Table VII. Summary of the characteristics of each receiver

Receiver number	Cooling method	Cell wiring	Average cell efficiency
1	Actively cooled by water	1P x 18S	10.3%
2	Actively cooled by water	3P x 6S	10.9
3	Actively cooled by water	1P x 18S 3P x 6S	11.8
4	Water cooled heat pipe	3P x 6S	10.8
5	Water cooled heat pipe	3P x 6S	11.5
6	Air cooled	3P x 6S	10.8

Table VIII. Summary of the characteristics of each optical module

Module number	Material	Reflecting surface	Light distribution
OM2A	Plexiglas	Aluminum	Large image spread
OM3A	Plexiglas	Aluminum	Good distribution
OM4A	Plexiglas	Aluminum	Medium image spread
OM5A	ABS	Aluminum	Rough surface, large image spread
OM7A	Plexiglas	Copper	Best distribution
OM8A	Plexiglas	Silver	Good distribution

As shown in Figure 5, each receiver fits into an optical module. Each optical module was made of ABS plastic or plexiglas. The correct shape was formed by heating the plastic and then pulling it by a vacuum into a mold. The reflective surfaces of each module were then coated with evaporated metal. Copper, silver, and aluminum were used in different modules. Table VIII summarizes the characteristics of the six optical modules. The relative light distribution information is courtesy of Arizona Scientific Research where the optical modules were made.

Electrical Measurements

During measurements, the modules were mounted on a polar type of mount normally used for telescopes. Modifications were made to handle the modules. A clock drive kept the module aimed at the sun once it was properly oriented. The initial orientation was done by measuring the module short circuit current and making adjustments until it was maximized. A photograph of the module on the clock driven mount is seen in Figure 15.

The module output current was determined by measuring the voltage drop across a 0.01 ohm precision resistor while the module voltage was measured directly from the module terminals. The precision resistor and a variable resistor were connected in series across the output terminals. An X-Y recorder was used to draw I-V characteristic curves of the module output. The curves were drawn by the recorder as the variable resistor was changed from zero to values large enough to complete the curve. Figure 16 shows a diagram of the apparatus used.

Figure 15. Module mounted on the clock driven telescope mount.

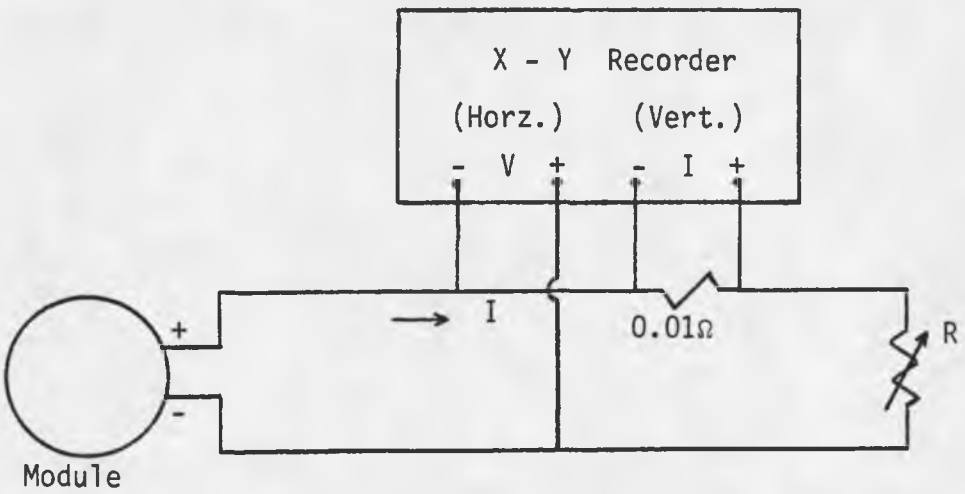

Figure 16. Module electrical test apparatus.

Electrical measurements were used to determine the relative quality of each optical module. The optical quality depends on the evaporated metal coating and the relative light distribution. The reflectance of the evaporated metals in order from best to worst are silver, aluminum, and copper. However the best to worst optical modules will not necessarily be in that order. Surface defects and abnormalities in the plastic due to inaccurate molding cause optical degradation.

In order to make comparisons between the optical modules, measurements were made with receiver #3 inserted in each of the six modules. Receiver #3 was used because it was expected to have the highest efficiency. I-V curves were taken with each module using the cells of receiver #3 in both the 1P x 18S and 3P x 6S wiring configurations. The data taken for each of the wiring configurations is represented in Tables IX and X. All current and power data has been adjusted for light input variations as if all the measurements were taken in a solar flux of exactly one sun or 100mW/cm^2. The calibrated standard cell was used to determine the exact solar intensity. The cross sectional area of the module was 0.38 square meters. Thus at one sun 380 watts of light was intercepted by the module. The module efficiency was determined by dividing the maximum delivered electrical power by 380 watts.

Module OM5A has a significantly lower efficiency in both cases. This module was the only one made of ABS instead of plexiglas. A visual inspection revealed that it did not mold well and has departures from smoothness that would contribute to a poor light distribution. Modules OM2A, OM3A, and OM4A were all made of plexiglas and used aluminum

Table IX. Adjusted data for each optical module with receiver #3 (1Px18S)

Module number	I_{sc}	V_{oc}	I_m	V_m	P_m	Power in	Eff.
OM2A	1.75A	12.4V	1.67A	11.0V	18.4W	380W	4.8%
OM3A	1.85	12.4	1.77	11.1	19.6	380	5.2
OM4A	2.70	12.4	2.57	10.0	25.7	380	6.8
OM5A	1.70	12.2	1.59	10.8	17.2	380	4.5
OM7A	2.92	12.5	2.75	10.2	28.1	380	7.4
OM8A	3.10	12.5	2.88	10.2	29.4	380	7.7

Table X. Adjusted data for each optical module with receiver #3 (3Px6S)

Module number	I_{sc}	V_{oc}	I_m	V_m	P_m	Power in	Eff.
OM2A	8.3A	4.0V	7.1A	3.2V	23.7W	380W	6.2%
OM3A	10.3	3.9	9.6	2.9	27.8	380	7.3
OM4A	10.2	3.9	9.1	3.0	27.3	380	7.2
OM5A	6.6	4.1	6.3	3.3	20.9	380	5.5
OM7A	10.1	4.0	9.3	3.1	28.8	380	7.6
OM8A	10.6	4.1	9.8	3.1	30.5	380	8.0

as the reflective surface. They were somewhat similar except that OM2A has a significantly lower efficiency due to a larger image spread. Silver is predicted to have a better reflectance than the other metals and indeed module OM8A had the highest efficiency. Module OM7A also had a relatively high efficiency. While copper's reflectance is not as good as silver or aluminum, module OM7A had a good light distribution which made it a good optical module.

If any one of the modules reflected an equal concentration of light on every cell, the 1P x 18S module efficiency would be the same as the 3P x 6S efficiency. However, if all cells in a 1P x 18S configuration are not uniformly illuminated, the module current is limited by the current generated by the cell with the least illumination. This decreases the module efficiency. In every module tested, the efficiency decreased as the cells were changed from 3P x 6S to 1P x 18S. This demonstrates the non-uniformity of concentrated light on the cells.

Once it was determined that the best optical module was OM8A, each of the six receivers was tested using it. I-V curves were taken with each receiver inserted into module OM8A. Table XI shows the resulting electrical results after the data was corrected to a solar intensity of 100mW/cm^2 (one sun).

There were several factors which determined the electrical efficiency of each receiver. The average efficiency of the cells on each receiver was important but two other factors had a significant influence. As observed with receiver #3, an unequal light distribution on the receivers due to imperfect optical modules made it more efficient to wire the cells in the 3P x 6S configuration. The final factor in

Table XI. Adjusted data for each receiver in optical module OM8A

Receiver number	Cell wiring	I_{sc}	V_{oc}	I_m	V_m	P_m	Power	Eff.
1	1Px18S	2.4A	12.7V	2.2A	11.0V	24.2W	380W	6.4%
2	3Px 6S	9.9	4.1	9.4	3.1	29.1	380	7.7
3	1Px18S	3.1	12.5	2.9	10.2	29.4	380	7.7
3	3Px 6S	10.6	4.1	9.8	3.1	30.5	380	8.0
4	3Px 6S	9.1	2.4	7.4	1.5	11.1	380	2.9
5	3Px 6S	10.3	3.2	8.7	2.2	19.1	380	5.0
6	3Px 6S	9.9	2.9	8.3	1.9	15.8	380	4.2

determining the efficiency of each receiver was the operating temperature of the solar cells. The low efficiencies of receivers #4, #5, and #6 were due to high cell temperatures caused by the heat pipe arrangements. High cell temperatures caused the cell voltage to drop significantly. This can be seen by observing the low voltages of receivers #4, #5, and #6 compared with the 3P x 6S voltage of receiver #3. The currents were not significantly changed.

The optical module-receiver combination with the best overall efficiency was optical module OM8A with receiver #3 wired in the 3P x 6S configuration. This combination used a module with silver as the reflective surface and had a relatively good image distribution. The average cell efficiency was highest of all receivers and the 3P x 6S cell wiring helped reduce any losses caused by unequal light distribution. The receiver was also actively cooled with water keeping the cells relatively cool and operating at higher efficiencies. Figure 17 shows

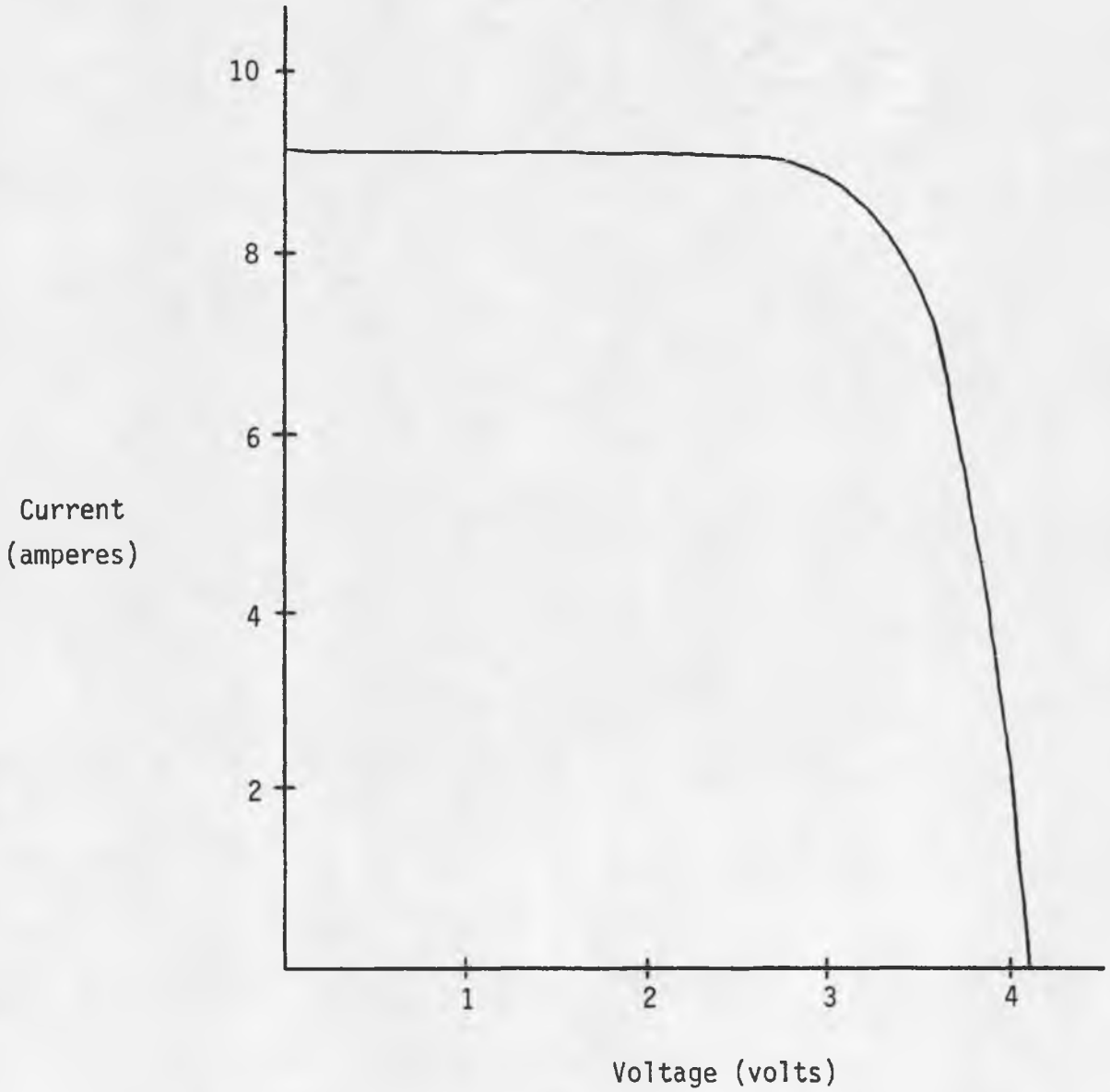

Figure 17. I-V curve using optical module OM8A with receiver #3 (3Px6S).

the I-V curve of this combination which gave the best electrical output. This curve shows the raw data before it was corrected to a solar intensity of one sun.

Temperature Measurements

All water cooling was provided from domestic water lines. In order to determine an adequate flow rate for an actively cooled receiver, cell temperature was measured as a function of flow rate. Receiver #3 and optical module OM8A were used in this experiment. As shown on the graph in Figure 18, the cell temperaure levels off after the flow rate was increased to three liters per minute. In order to be sure that the cell temperatures had indeed leveled off, it was decided to use a flow rate of four liters per minute in all cases.

Temperature measurements were taken with each receiver in optical module OM8A. Thermocouples were attached to several places on each receiver allowing temperatures to be monitored at a variety of locations. While temperature measurements were being taken, the module short circuit current was also being monitored. The short circuit current was kept maximized to ensure that the module orientation was such that a maximum of solar radiation was reaching the receiver. Table XII summarizes the results of the temperature measurements taken.

As can be seen, direct water cooling used in receivers #1, #2, and #3 is far superior to cooling with heat pipes which were used in receivers #4, #5, and #6. Heat pipe cooling allowed the cell temperatures to go well above 100^{o}C. The higher cell temperatures in these modules are due to the large temperature drops at the interface between the heat pipe and the two end pieces which surrounded the heat

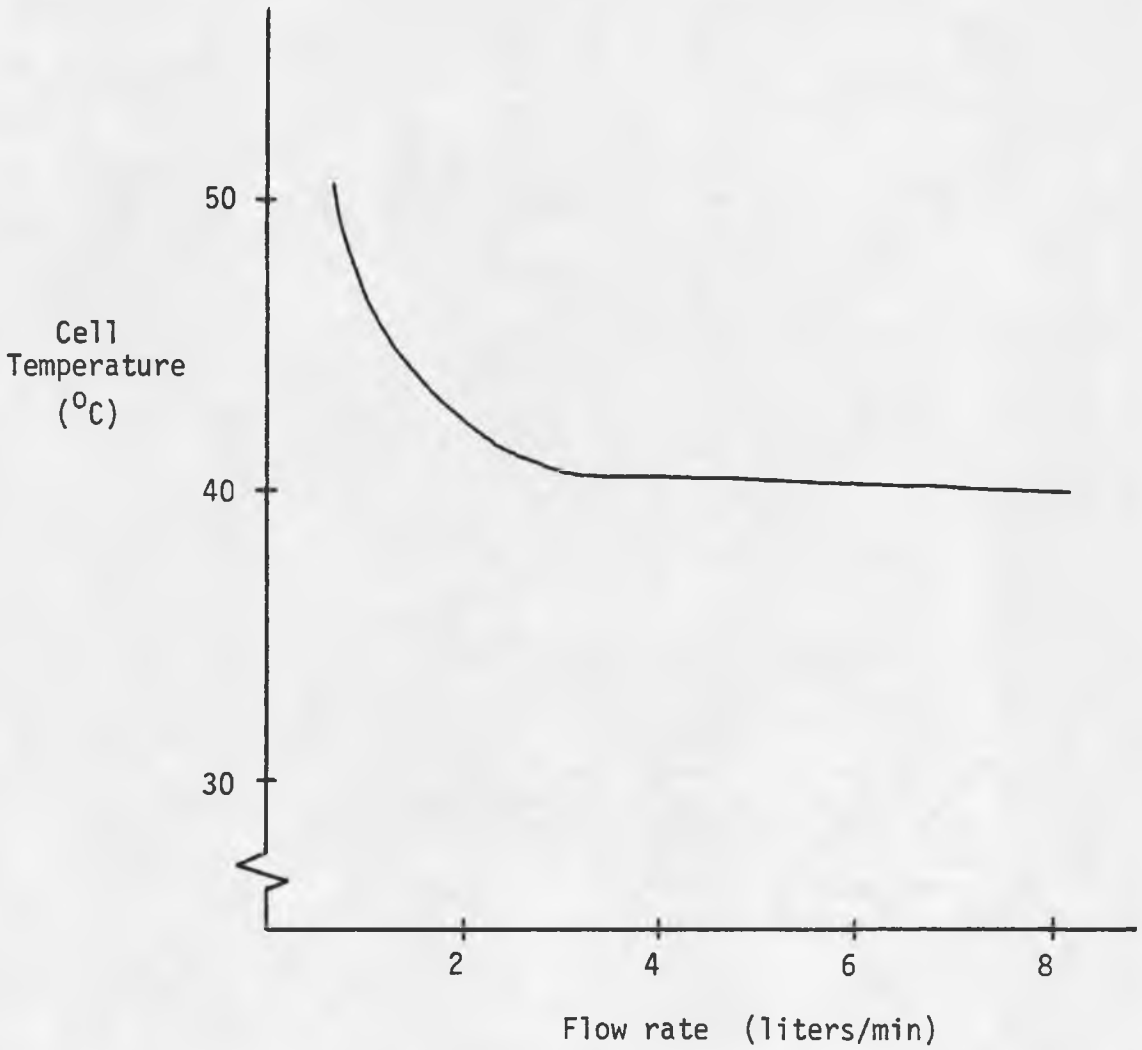

Figure 18. Cell temperature versus flow rate on an actively cooled receiver.

pipe as well as the temperature drop across the heat pipe itself. Any air pocket around the heat pipe would severely hamper the flow of heat. It should be noted that it did not seem to make any difference whether the bottom end of the heat pipe was actively or passively cooled. Receiver #6 had the only heat pipe that was passively cooled with air fins. Heat pipes in general are totally inadequate for cooling solar concentrators with intensities of 40 suns. One optimistic observation is that the very high receiver temperatures did not appear to damage the silicone rubber adhesive used in mounting the cell-molybdenum combination onto the receiver. The soldered interconnections were also not affected by the high temperatures.

Table XII. Temperature measurements with each receiver in optical module OM8A

Receiver number	Cooling water	Receiver surface	Solar cell	ΔT Cell to receiver	ΔT Receiver to water	ΔT Cell to water
1	20°C	27°C	47°C	20°C	7°C	27°C
2	24	32	47	15	8	23
3	23	30	43	13	7	20
4	27	140	190	50	113	163
5	22	116	140	24	94	118
6	--	---	138	--	--	119*

* Since receiver #6 was passively air cooled, this temperature represents the ΔT between the cell and the ambient air.

Active water cooling kept the cell temperatures below 50°C. The cell temperature on these receivers degraded the module voltage by only a minimal amount. In general, the temperature measurement results of the three actively cooled are encouraging. The actual cell temperatures, as well as the temperature difference between the cells and the receiver, are very close to the measurements taken using the solar simulator. The module temperatures were what would have been predicted.

The overall electrical efficiencies of receivers #4, #5, and #6 are relatively low. This is because of the degradation in voltage due to high cell temperatures. In order to see exactly how much the voltage was degraded, measurements were taken of the module open circuit voltage versus cell temperature. Receiver #4 in optical module OM8A was used for this test. The module was shaded until the cells had reached a relatively cool temperature and then suddenly exposed to the full sun. The open circuit voltage and the cell temperature were measured as the receiver temperature gradually increased. The curve of V_{oc} versus cell temperature is shown in Figure 19. The average slope of the plot is -11.5mV/°C. Since the cells are wired in the 3P x 6S configuration, this translates to a voltage loss of -1.92mV/cell·°C which is close to what was expected.

Optical Analysis

The overall efficiency of a module is determined by a number of different factors. These factors were examined using the combination of receiver #3 in optical module OM8A. The module electrical efficiency can be represented by equation (7).

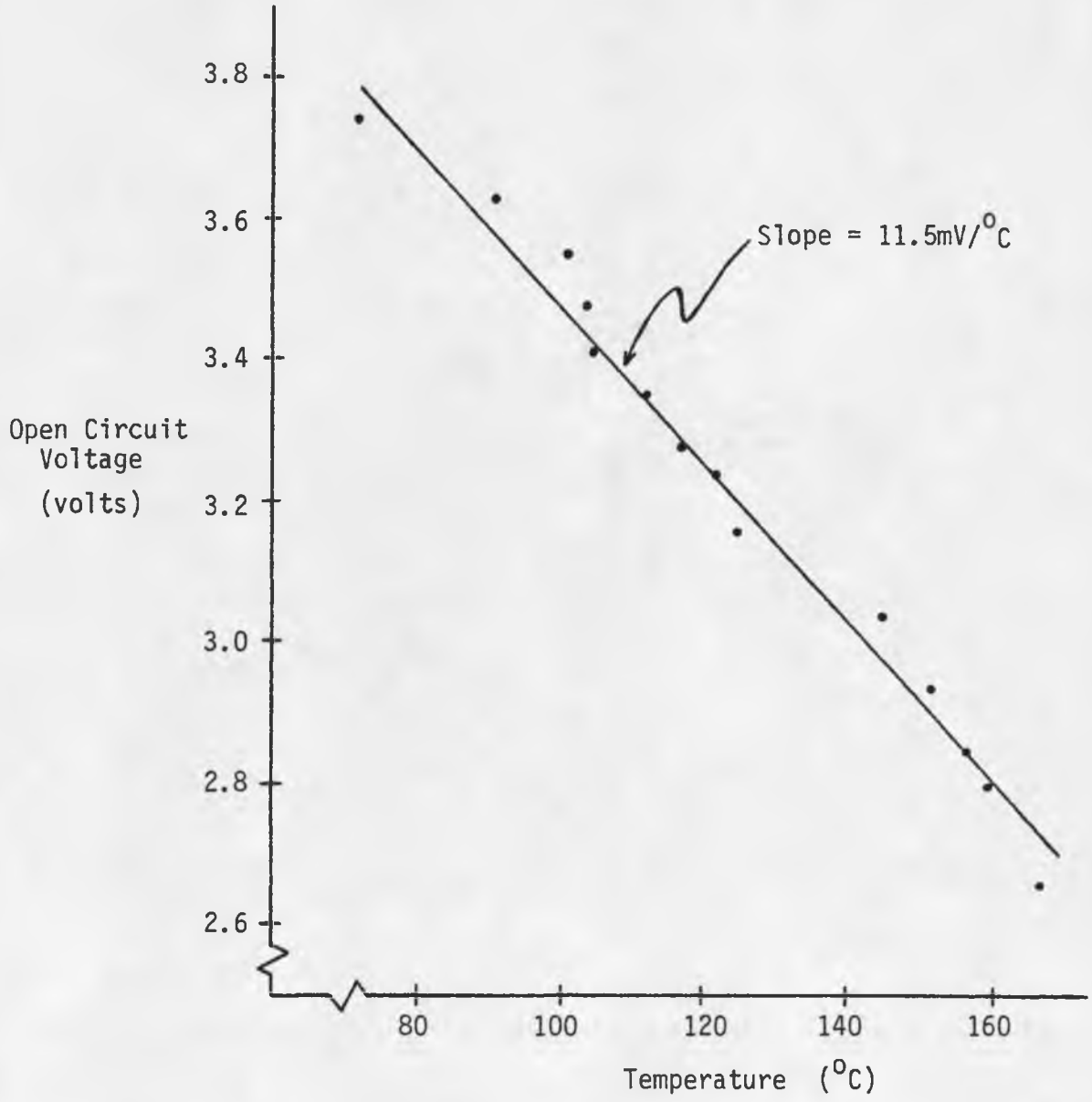

Figure 19. Module V_{oc} versus cell temperature.

$$\eta_{module} = T_{dome} \cdot \eta_{geom} \cdot R_{Ag} \cdot \eta_{opsp} \cdot \eta_{cd} \cdot \eta_{cell} \qquad (7)$$

T_{dome} is the transmission coefficient for the plastic dome cover which protects the reflecting silver as well as the cells from the environment. This can easily be determined by taking similar measurements with and without the dome cover. It was already determined that with exactly one sun the 1P x 18S configuration had a maximum electrical power of 29.4 watts with the dome on. With the dome off, the electrical power was 31.5 watts. Since the power is proportional to the solar intensity, T_{dome} could be calculated to be 0.93.

The geometric efficiency of the module is denoted by η_{geom}. By studying Figure 5, one can see that the incoming rays in the center of the module will strike the receiver and the flange where the receiver is connected to the reflector. This light will not have a chance to be reflected onto the solar cells and will be lost. The cross sectional area of the module is 0.380 square meters while the cross sectional area of the receiver and flange is 0.018 square meters. Thus, 5% of the light which shines through the dome never even strikes the reflector; thus η_{geom} is 0.95.

η_{opsp} is the optical spread function. There are two factors which determine η_{opsp}. The first is that some of the reflected light will strike the receiver, either too high or too low, missing the cells. The second factor that determines η_{opsp} is the uniformity of light on the receiver. A photovoltaic system operates most efficiently when all cells are illuminated equally. The value of η_{opsp} is to be determined. R_{Ag} is the reflectivity of the optical module used which was a silvered front-surface mirror. The value for R_{Ag} is typically 0.95.

The final two factors which determine the overall module efficiency are the cell density and the average cell efficiency of the module. The average cell efficiency η_{cell} of the module was determined to be 11.8% or 0.118. The cell density η_{cd} is the percentage of area on the receiver where light is supposed to shine that is actually covered by solar cells. This is kept from being 1.00 by the small spaces that must exist between adjacent solar cells. η_{cd} was 0.95.

It was already determined that the overall efficiency of optical module OM8A with receiver #3 wired in the 3P x 6S configuration is 8.0%. Knowing this, all other known values can be substituted into equation (7) and η_{opsp} solved for. In this case, the optical spread function was determined to be 0.85. With more accurate tooling and manufacturing techniques, η_{opsp} could be improved to somewhere between 0.90 and 1.00, say 0.95. Concentrator cells with an efficiency of 20% should also be available within a few years. With these improvements, a module of this design could have an efficiency of 14.7%.

In order to get a clearer picture of how optical module OM8A was performing, a scan of the illumination on the receiver was made. This was done by removing the plastic dome cover of the module and measuring the short circuit current of each individual cell. Each value of current measured was multiplied by 0.93 to correct it to what the short circuit current would have been if the cover dome had been in place. This value was then compared to the short circuit current for that particular cell measured using the solar simulator at 40 suns. From these two values, the average solar intensity falling on each cell was calculated. Table XII summarizes the results. The short circuit

current multiplied by the 0.93 correction factor and the average solar intensity on each cell are included in the table. The measurements were taken in a solar intensity of exactly one sun so no adjustments were needed to correct for the incoming solar intensity.

Table XIII. Optical data of optical module OM8A with receiver #3

Side	1	2	3	4	5	6	Cell position
I_{sc}	4.15A	3.65	4.00	3.10	2.90	3.70	Top
Solar intensity	44 suns	39	45	33	31	41	
I_{sc}	4.70A	4.15	4.80	4.55	3.20	4.30	Middle
Solar intensity	51 suns	45	52	49	33	47	
I_{sc}	3.80A	3.40	3.30	3.25	2.90	3.65	Bottom
Solar intensity	42 suns	36	36	34	31	41	

The module was designed to deliver a solar concentration of 40 suns to every cell. In reality, the average solar concentrations on each cell ranged from 31 suns to 52 suns; the solar intensity across all cells in the module averaged out to be 40 suns. As one might expect, the highest light intensity on each side was on the middle cell. From the middle of each side the solar intensity decreases as one went up or down.

The solar intensities on side 5 were, in particular, very low. The probable causes are defects in the reflecting surface or deformities in the plastic on which the silver had been deposited. If the cells on this receiver were wired in the IP x 18S configuration, the top and bottom cells on side 5 should limit the module short circuit current to 2.90 amperes.

In reality, the short circuit current for this configuration was 3.10 amperes. If the 3P x 6S wiring was used, side 5 should limit the module short circuit current to 9.00 amperes. The actual short circuit current for this case was 10.6 amperes.

Although a maximum module efficiency of only 8.0% has been realized, an in depth study of the modules has shown where improvements can be made. For modules of this design, active cooling must be used to keep the cell temperatures reasonably low. Improvements in the optics and in cell efficiencies could improve the overall efficiency to 15% in a concentrator of this design.

CHAPTER VI

CONCLUSIONS AND RECOMMENDATIONS

Results and Observations

Although the receivers and optical modules were constructed by Arizona Research, all the other steps in the fabrication of the segmented dish concentrator module were performed at the University of Arizona. Several different methods of cell mounting were investigated. A mounting procedure was selected which gave adequate heat conduction and provided for convenient electrical connections between cells. Once the modules were put together, extensive tests were carried out to determine the electrical performances of the modules and the efficiencies of various types of heat sinking. The optical efficiency of one module was also studied.

A considerable amount of time was spent in determining the best way cells could be mounted in a module. In order to make electrical connections to the back side of a cell after it was mounted, cells were first mounted on electrically conducting substrates. Molybdenum was chosen because it has a thermal coefficient of expansion similar to that of silicon. Before soldering the cells onto the molybdenum substrates, the cells were electroplated with copper to protect the silver metalization. The molybdenum was electroplated with nickel because solder will not adhere to molybdenum.

The next task was to determine the best adhesive and the best method for mounting the cell-substrate combination onto the receivers. Two qualifications had to be met. All of the molybdenum substrates

needed to be kept electrically insulated from the receiver on which they were mounted. The electrical performance of a module would be severely degraded if any shorts existed. Besides being electrically insulating, the adhesive must also be a good conductor of heat. As observed in the modules with poor heat sinking capabilities, the module voltage decreases significantly when the cells are forced to operate at high temperatures. A good adhesive allows heat to pass freely from the cell to the receiver. If the receiver is a good heat sink, the heat generated by the sunlight on the cells can be dissipated quickly allowing the cell temperature to remain relatively low.

An indoor solar simulator capable of generating light intensities of up to 50 suns was used in performing a variety of thermal tests. Thermocouples were used to measure temperatures wherever desired. By measuring temperature differences across various adhesives, the best heat conductors could be identified. A smaller temperature difference means a better conduction of heat. Heat conduction was not the only criterion used in selecting an adhesive. The adhesive was also judged on its quality of adhesion as well as the relative ease with which it could be used. Electrically conducting adhesives were not even considered. After a considerable amount of testing, silicone rubber mixed with powdered silicon in a 1:1 ratio by volume was selected. Tests with this adhesive in the solar simulator show that in a light concentration of 40 suns there will be a temperature difference of about 17^{o}C between the cell and a water cooled heat sink. The temperatures measured in the completed modules with actively cooled receivers gave the same results.

After being mounted on molybdenum, every cell was electrically tested under a solar intensity of 40 suns. There were two reasons for doing this. Although the cells were designed to operate under an intensity of 40 suns, it was necessary to be sure that they performed adequately before mounting them in modules. The efficiency of every cell was also determined so that cells with similar efficiencies could be mounted on the same receiver. The cell efficiencies were fairly uniform. Although they ranged from 9.6% to 12.2%, most cell efficiencies were near 11%. The average cell efficiency at 40 suns for all cells was exactly 11.0%.

The cell-substrate combinations were mounted onto the six receivers using the mixture of silicone rubber and silicon powder. The electrical performance of every receiver was then analyzed. Receiver #3 wired in the 3P x 6S configuration gave the best electrical performance. This is what would be expected. The average cell efficiency was the highest of any receiver. It was also actively cooled, keeping voltage losses due to high cell temperatures to a minimum. The 3P x 6S wiring lessened the losses due to non-uniform light distribution on the receiver.

Temperature measurements show that heat sinking the receivers with heat pipes is inadequate. The heat can not be dissipated quickly enough and cell temperatures go well above 100^{o}C. The effects of these high temperatures are seen in the low electrical outputs of these receivers. Although the module current was not effected, the voltage was decreased by a significant amount. On the other hand, the receivers which were actively cooled kept the cell temperatures below 50^{o}C. Voltage degradation is not a severe problem in this temperature range. The

temperature differences between the cells and the actively cooled receivers ranged from 13°C to 20°C. The thermal tests using simulated solar light predicted this temperature difference to be 17°C.

Using electrical measurements, optical module OM8A was determined to have the best overall optical efficiency. This module had a relatively good image distribution in comparison to the other modules and used a highly reflective coating of evaporated silver as the reflecting surface. This optical module was analyzed in detail to get a better picture of its optical performance. This study revealed that even the optical module with the best overall optical performance had a non-uniform distribution of light across the cells on the receiver. This alone can contribute significantly to a degradation in the electrical output of a module.

Recommendations for Module Improvement

The modules fabricated by the techniques described in this report have promising output capabilities. However, there is room for improvement in several areas. These include cell mounting procedures, heat sinking techniques, and an improvement in the quality of some of the components which make up the concentrator.

Although a mixture of silicone rubber and silicon powder performed adequately in conducting heat from cell to receiver, there is room for improvement. Under a light concentration of 40 suns a temperature difference between cell and receiver of 17°C was observed. It would be very desirable if this temperature difference could be lowered to 10°C or less. Experiments and more research in this area could reveal that there

is an electrically insulating adhesive which conducts heat better than the compound used here.

There are many steps in the technique developed for mounting the cells onto the receivers. The process is rather difficult and time consuming. This translates to a very high labor cost if these collectors are to be mass produced for the commercial market. The large number of steps in the mounting process also makes it possible for more things to go wrong. It would be desirable to develop a mounting procedure more efficient and easier than that described in this report.

It will probably always be necessary to mount the cells on an electrically conductive substrate such as molybdenum in order to be able to make electrical connections to the back side of the cells. However, if the receivers could be constructed of a material that is an electric insulator yet conducts heat well, the mounting procedure would be simplified. A great amount of effort was taken to ensure that the molybdenum substrates remained electrically isolated from the receiver. Eliminating this need would simplify the whole mounting procedure. It would also make it possible to use electrically conductive adhesives which are likely to have better heat conducting capabilities.

The best receiver used together with the best optical module gave an overall electrical efficiency of only 8.0%. This leaves room for a lot of improvement in the performance of the solar collector. Of all the factors which determine the overall electrical efficiency, the

two which can be improved the most are the cell efficiency and the optical spread function of the modules.

Even optical module OM8A, the best of the optical modules tested, had a relatively non-uniform distribution of light across the 18 cells on the receiver. This module had an optical spread function of 85%. Thus, there is room for improvement in the performance of the optical modules. If the overall performance of this solar concentrator is to be improved, time and energy should be directed toward improving the process used in fabricating the optical modules. If the optical performance of these modules can approach what is theoretically expected of them, the optical spread function would be near 100%. The optical modules used in this project were part of a small order delivered by Arizona Scientific Research. If mass produced, the optical performance of the modules would probably improve significantly.

The cells used in the modules had an average efficiency of 11.0%. By today's standards, that is not particularly good. In the near future photovoltaic concentrator cells should be available with efficiencies near 20%. These cells used together with significantly improved optical modules could result in an overall collector efficiency of almost 15%. This means that the actual electrical output would be 55 watts which is considerably higher than the electrical outputs which were observed. If a module efficiency of 15% can be achieved, there is reason to be optimistic in the future of solar concentrators of this type.

REFERENCES

Backus, C.E., Jacobson, D.L., McNeil, B.W., and Wood, B.D. Terrestrial Photovoltaic Power Systems With Sunlight Concentration Annual Progress Report - 1977. Issued by Sandia Laboratories, Albequerque, N.M., May 1978.

Gray, A.G. . Modern Electroplating . New York: John Wiley and Sons, Inc., 1953.

Handbook of Chemistry and Physics Cleveland: CRC Press, 1974.